ARTICLE IN PRESS

KICS The Korean Institute of Communications and Information Sciences

Available online at www.sciencedirect.com

ScienceDirect

ICT Express xxx (xxxx) xxx

www.elsevier.com/locate/icte

Trustworthy handover in LEO satellite mobile networks

Soyi Jung[a], Moon-Sik Lee[b], Jihyung Kim[b], Mi-Young Yun[b], Joongheon Kim[c,*], Jae-Hyun Kim[d,*]

[a] School of Software, Hallym University, Chuncheon, Republic of Korea
[b] Electronics and Telecommunications Research Institute (ETRI), Daejeon, Republic of Korea
[c] School of Electrical Engineering, Korea University, Seoul, Republic of Korea
[d] Department of Electrical of Computer Engineering, Ajou University, Suwon, Republic of Korea

Received 15 July 2021; received in revised form 3 October 2021; accepted 28 October 2021
Available online xxxx

Abstract

Recently, a low earth orbit (LEO) satellite network is one of major systems to provide seamless access for terrestrial network systems. In order to provide robust access, efficient handover mechanisms are essential. However, conventional mechanisms may introduce frequent handovers due to the rapid movement of satellites. To deal with this problem, this paper proposes a learning-based auction handover under the consideration of received signal strength and service time between terrestrial users and satellites. The reason why auction-based approach is utilized is that it is generally considered as trustworthy. Our experiment results verify the proposed algorithm achieves desired performance.

Keywords: LEO satellite; Handover; Myerson auction; Deep learning

1. Introduction

Compared with medium earth orbit (MEO) and geostationary earth orbit (GEO) satellites, low earth orbit (LEO) satellites provide promising configurations to achieve lower propagation latency and higher throughput. However, due to the rapid movement of LEO satellites and terrestrial users (TUs), frequent handovers are inevitable. Moreover, these frequent handovers introduce considerably negative impacts on the quality of service (QoS) in LEO satellite networks (LSNs) [1,2].

Recently developed research contributions are focusing on the handover strategies with centralized management. To realize flexible satellite handovers, a graph-based handover framework is designed to solve a path-finding problem using reinforcement learning [3]. In addition, a potential game-based handover algorithm is proposed to guarantee balanced constellation network load [4]. Furthermore, a novel LEO handover algorithm using estimation theory-based forecasting is also proposed [5]. Even though these algorithms achieve performance improvements, it has no considerations on truthfulness (e.g., revenue, credibility, etc.). Furthermore, they are disadvantageous in terms of scalability (e.g., signaling overheads) due to centralized computation.

In order to solve handover problems in a distributed manner, this paper designs an algorithm based on econometric approach, i.e. auction, for providing distributed utility maximization as well as truthfulness/trustworthy [6]. Among major well-known auction algorithms, Myerson auction is one of efficient revenue-optimal single-item auctions [7]. In our proposed auction-based LEO satellite handover mechanism, each TU makes a decision for LEO satellite handover to prevent indiscriminate attempts by selfish users. In auction, each TU performs auction-based handover decision computation by announcing bidding as an auctioneer. Then, multiple nearby LEO satellites will join the auction procedure when they (i.e., candidate LEO satellites) are willing to join based on their own utility computation. Then, individual candidate LEO satellites will prepare their own bids based on (i) received signal strength and (ii) service time. Then, one satellite among candidate LEO satellites will be a winner by the auction procedure that is called second price auction (SPA). The reason why SPA is considered among various auction algorithms is that it is generally considered as truthful/trustworthy [6]. However, one of main drawbacks of SPA is that it is not revenue-optimal. In order to improve the revenue (i.e., enhancing the benefits of

* Corresponding authors.
E-mail addresses: sjung@hallym.ac.kr (S. Jung), moonsiklee@etri.re.kr (M.-S. Lee), savant21@etri.re.kr (J. Kim), myyun@etri.re.kr (M.-Y. Yun), joongheon@korea.ac.kr (J. Kim), jkim@ajou.ac.kr (J.-H. Kim).
Peer review under responsibility of The Korean Institute of Communications and Information Sciences (KICS).

https://doi.org/10.1016/j.icte.2021.10.011

the seller/TU), a deep learning based solution computation is used in this paper.

Finally, it can be noted that our proposed handover algorithm works as a form of distributed and trustworthy computation according to deep learning-based SPA-grounded mechanism design.

The main contributions of this paper are as follows.

- First, to the best of our knowledge, this work is the first contribution which considers trustworthy handover in satellite aerial networks.
- Next, the proposed algorithm is fully distributed, i.e., scalable operations can be realized.
- Lastly, thanks to the use of auction-based algorithms, the proposed algorithm guarantees optimal revenue as well as enables self-configurable operations for adapting various conditions.

2. LEO satellite handover decision criteria

Our considered satellite network consists of LEO satellites and TUs. We consider an LSN that provides seamless Internet access service to individual TUs. Each TU is covered by multiple LEO satellites simultaneously. Once a TU accesses LSNs, the TU will be allocated with multiple candidate satellites. In conventional satellite networks, frequent handovers will be triggered due to the random movements of TUs (e.g., unmanned aerial networks [8,9]), which would finally lead to high handover failure rates. In order to avoid this behavior, we consider two handover criteria, i.e., received signal strength and service time.

- *Received signal strength:* The TU measures every received signal strength indicated (RSSI) of individual LEO satellites and selects the strongest data link [5]. More details are in Section 2.1.
- *Service time:* The short association between TUs and LEO satellites can increase the number of handover frequencies. The TU selects the satellites that offer maximum service time [10]. More details are in Section 2.2.

According to the proposed auction-based handover, the signaling overheads can be reduced because gathering handover-related information from all LEO satellites in world-wide is not needed, whereas the information from all LEO satellites should be gathered in centralized algorithms.

2.1. Received signal strength

The sum of pathloss can be calculated and predicted by the movement patterns of TUs and the orbits of LEO satellites. The received power is given by,

$$P_R = P_T \cdot G_T \cdot G_R \cdot G, \tag{1}$$

where P_T is a transmission power, G_T and G_R are the antenna gains of the transmitter and receiver, and G is a channel model, respectively. The channel model G between an LEO satellite i and a TU j consists of the pathloss PL, pitch angle fading G_H, atmospheric fading A, and Rician small-scale fading φ [11], as follows,

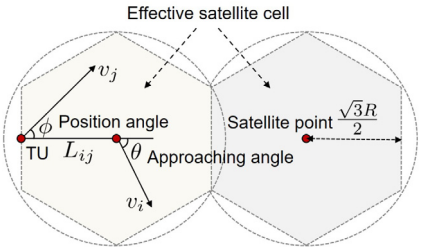

Fig. 1. A motion relationship between a TU and an LEO satellites.

$$G = PL \cdot G_H(\psi_{ij}) \cdot A(d_{ij}) \cdot \varphi, \tag{2}$$

where ψ_{ij} is a pitch angle and d_{ij} is a propagation distance between TUs and satellites. For the TU j located in (x_j, y_j) covered by the beam of an LEO satellite i. The pitch angle ψ_{ij} can be calculated as,

$$\psi_{ij} = 2 \arctan \frac{\sqrt{(x_j - o_{i,1})^2 + (y_j - o_{i,2})^2}}{2h}, \tag{3}$$

where h is the altitude of satellites, $(o_{i,1}, o_{i,2})$ is the center position of the coverage region of i. The propagation distance d_{ij} between a satellite and a TU is given by,

$$d_{ij} = \sqrt{h^2 + (x_j - o_{s,1})^2 + (y_j - o_{s,2})^2}, \tag{4}$$

where $(o_{s,1}, o_{s,2})$ is the position below satellite. The pathloss is expressed as,

$$PL = \left(\frac{c}{4\pi d_{ij} f_c}\right)^2, \tag{5}$$

where c and f_c are the speed of light and the carrier frequency. The pitch angle fading [12] is given by,

$$G_H(\psi_{ij}) = Ap_{\text{eff}} \cdot cos(\psi_{ij})^{\eta} \frac{32log2}{2\left(2\arccos\left(\sqrt[\eta]{0.5}\right)\right)^2}, \tag{6}$$

where Ap_{eff} is an antenna aperture efficiency, η is the roll-off of the antenna. The atmospheric fading is given by,

$$A(d_{ij}) = 10^{\left(\frac{3d_{ij}\chi}{10h}\right)}, \tag{7}$$

where χ is the attenuation through the clouds and rain in dB/km.

2.2. Service time

The relative azimuth value P_a and relative distance change value P_d between a TU and an LEO satellite are adopted to describe the spatial relationship. We assume that L_{ij} is a connecting line between i and j. As shown in Fig. 1, ϕ and θ are denoted as the position angle and approaching angle respectively, where $0 \le |\phi| \le \pi$ and $0 \le |\theta| \le \pi$. Define that the clockwise direction is positive, vice versa. The normalized angle can be as,

$$P_\phi = 1 - \frac{2|\phi|}{\pi}, \quad P_\theta = \frac{2|\theta|}{\pi} - 1, \tag{8}$$

Table 1
Parameters related LEO satellite system.

Variables	Descriptions
Altitude of LEO satellite	1500 km
LEO satellite antenna factor	20
Velocity of TUs	5 m/s
Transmitter power of LEO satellite	10 dBW
Noise power spectral density	−173 dBm/Hz
Rician small scale fading	20 dB
Carrier frequency	Ka band (30 GHz)

where P_ϕ is the normalized of ϕ and P_θ is a normalized θ. Therefore, the relative azimuth value P_a can be obtained as,

$$P_a = 2 + \frac{P_\phi + P_\theta}{2}. \tag{9}$$

The speed projection difference for the direction of L_{ij} is v_{ij} which can be denoted as,

$$v_{ij} = v_i \cos\theta + v_j \cos\phi, \tag{10}$$

where v_i and v_j are the speed of a satellite and a TU. If satellites are close to a TU, v_{ij} will be negative value, and vice versa. We define that the relative distance variation value $P_{\Delta D}$ to transform v_{ij} into a positive value.

$$P_{\Delta D} = 2 - \frac{v_{ij} d_{ij}}{R(v_i + v_j)}, \tag{11}$$

where $-v_i - v_j \le v_{ij} \le v_i + v_j$, and R is the radius of the satellite coverage. The maximum effective radius is $\frac{\sqrt{3}R}{2}$ because the effective cell is hexagon for ultra-dense constellation [13]. Therefore, the normalized effective relative distance can be calculated as,

$$P_D = \begin{cases} 1, & \text{if } d_{ij} \le \frac{\sqrt{3}R}{2}, \\ \frac{R - d_{ij}}{R}, & \text{otherwise.} \end{cases} \tag{12}$$

The relative distance change value P_d is calculated as $P_d = P_{\Delta D} \cdot P_D$. To give an overall assessment for spatial relations, we define P_{ij} as the spatial relationship which combines P_a and P_d,

$$P_{ij} = \begin{cases} \underbrace{\left(2 + \frac{P_\phi + P_\theta}{2}\right)}_{P_a} \cdot \underbrace{\left(2 - \frac{v_{ij} d_{ij}}{R(v_i + v_j)}\right)}_{P_d}, & \text{if } d_{ij} \le \frac{\sqrt{3}R}{2}, \\ \underbrace{\left(2 + \frac{P_\phi + P_\theta}{2}\right)}_{P_a} \cdot \underbrace{\left(\frac{R - d_{ij}}{R}\right)\left(2 - \frac{v_{ij} d_{ij}}{R(v_i + v_j)}\right)}_{P_d}, & \text{otherwise.} \end{cases} \tag{13}$$

3. Auction design via deep learning

3.1. Second price auction

Our proposed handover mechanism will be triggered when a TU initiates handover procedure. When a TU determines that handover is required, then the *request* message will be announced to nearby multiple LEO satellites. Among them, when the LEO satellites are willing to join the auction competition, they will organize their own bids based on the received signal strength (refer to Section 2.1) and service time (refer to Section 2.2). Here, the bid b_i of LEO satellite i can be computed as,

$$b_i \triangleq \alpha \cdot P_R + \beta \cdot P_{ij}, \tag{14}$$

where α and β stand for the normalized factors for received signal strength and service time, respectively. Note all parameters are in Table 1. Note that our bid will be increased when both values are increased.

Based on the submitted bid values, the TU will determine one winner (i.e., winning LEO satellite to provide Internet access services to the TU) which submitted the highest bid. Then, the winner will be selected to provide services and the payment equals the bid value which is the second highest. This is the detailed procedure of our proposed SPA-based handover mechanism.

Note that SPA is widely used for various distributed resource allocations because it is trustworthy [6].

3.2. Deep learning framework

In this section, a deep learning framework is designed and implemented in order to improve revenues in auctioneers/TUs. The reason why revenue improvements are required is that SPA is not revenue-optimal even though it is trustworthy [6]. According to deep learning-based SPA, our proposed mechanism can be trustworthy and revenue-optimal [14]; where the optimality stands for the improved revenue in terms of the auctioneer. As discussed in [14], the bid set of $d_i, i = \{1, \ldots, \mathcal{D}\}$ is converted to $\overline{b_i} = \phi_i(b_i), i = \{1, \ldots, \mathcal{D}\}$. Here, $\overline{b_i}$ means the transformed bid of d_i. The ϕ should have monotonicity which converts b into transformed bid $\overline{b}$.

The deep learning based SPA consists of three networks, i.e., monotonic network, allocation network, and payment network, where the monotonic network is for improving revenues based on given bids, the allocation network is for determining a winner LEO satellite, and the payment network is for the payment by the winner. More details about this learning-based SPA are discussed in [6].

The monotonic network (which is for sampling to increase revenues) is expressed as,

$$\overline{b_i} = \phi_i(b_i) = \min_{1 \le g \le \mathcal{G}} \left\{ \max_{1 \le u \le \mathcal{U}} (w^i_{g,u} b_i + \beta^i_{g,u}) \right\}, \tag{15}$$

where $w^i_{g,u}$ and $\beta^i_{g,u}$ are training parameters; weight and bias, respectively.

The allocation network (which is for selecting one winner) is mainly designed with softmax function, and it can be expressed as,

$$g_i = \texttt{softmax}\left(\overline{b_1}, \ldots, \overline{b_\mathcal{D}}; k\right) = \frac{e^{k\overline{b_i}}}{\sum_{j=1}^{\mathcal{D}} e^{k\overline{b_j}}}. \tag{16}$$

In auction, the payment of d_i becomes the value between the second highest bid and b_i if d_i becomes the winner. The non-negative set that is the result of `ReLU` function is considered in order to obtain the second highest bid. This

Table 2
Parameters related auction design via deep learning.

Variables	Descriptions
Learning rate	0.0001
L_2 regularization parameter	0.001
Training set size	400000 bid sets
Simulation epoch	1000
Number of TUs	5
Number of LEO satellites	16
Number of groups and units	5, 10
Approximate quality k	1, 2, 3

Table 3
Revenue statics (in Fig. 2)

	Bid	SPA-0	$k=1$	$k=2$	$k=3$
Mean	8.2925	6.7893	7.0717	6.9353	6.8213
Top 25%	9.5314	8.1682	8.3328	8.2810	8.2186

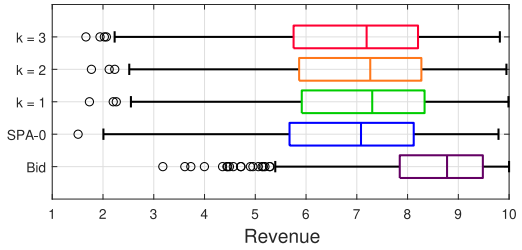

Fig. 2. Revenue statistics.

is basic concept to design payment network and it can be expressed as,

$$\overline{p_i} = \mathtt{ReLU}\left\{\max_{j\neq i}\left(\overline{b_i}\right)\right\}. \tag{17}$$

Finally, the inverse transformation that determines the payment of winner and its result is used as an input of (17), i.e.,

$$p_i = \phi_i^{-1}(\overline{p_i}) = \max_{1\leq g\leq \mathcal{G}}\left\{\min_{1\leq u\leq \mathcal{U}}(w_{g,u}^i)^{-1}(\overline{p_i} - \beta_{g,u}^i)\right\}, \tag{18}$$

where it calculates the actual payment of the winner.

4. Performance evaluation

The performance of our auction with deep learning is evaluated via data-intensive experiments. For the first experiment, the simulations work with various k that is the coefficient which determines the approximation quality (or sensitivity) of deep learning; and then the results are presented in terms of winning bid values and payments. This experiment includes the statistical results of SPA-0 (where SPA-0 means the SPA where the bids are non-negative), and the results are compared with our proposed mechanism. Therefore, the revenue-optimality of our mechanism will be presented. Our simulation settings include 5 TUs and 16 LEO satellites, and it will be training data for deep learning computation. Note all parameters are summarized in Table 2.

Fig. 2 and Table 3 show experiment results which compare the statistical payment values for each model while updating approximation parameter k in (16). In the experimental results of Fig. 2, the revenue stands for the expected income/earning at a TU. Thus, it can be interpreted as the income of a TU by selecting LEO satellite. Therefore, the performance of LEO satellite can be improved. The evaluation uses validation data when k are 1, 2, and 3. Fig. 2 shows the bid of winner, average payment, maximum payment, and minimum payment. As k increases, the gap between the average bid of winner and the average payment gets larger, i.e., 1.220841 ($k=1$), 1.357208 ($k=2$), and 1.471152 ($k=3$). When $k=3$, the gap between our proposed algorithm and SPA-0 is about 0.1 in terms of average whereas the gap is 0.3 when $k=1$. This result verifies that the model with $k=1$ takes the highest revenue. It can be seen that the revenue of auctioneer degrades in the order of $k=1$, $k=2$, $k=3$, and SPA-0, with the gap of 0.1.

In Fig. 3, experiment results are presented when selfish users are involved in handover trading. The selfish user is defined as a user which is always bidding with indiscriminate high values; and eventually it gives impacts to the others. This experiment conducts with the models of $k=1$ and $k=2$. The bidding value by selfish user is set to 8.35 and this is based on experiment results in Fig. 2, i.e., top 25% payment value with $k=1$ model. This experiment utilizes two scenarios, i.e., (i) 1 selfish user and 4 truthful users [i.e., Scenario (1) or S(1) in Fig. 3(b)]; and (ii) 5 truthful users [i.e., Scenario (2) or S(2) in Fig. 3(b)]. The left four bars in Fig. 3(a), i.e., [1–4], show the average utility values of selfish user when the selfish user becomes winner in auction in Scenario (1) when k varies. On the other hand, the right four bars in Fig. 3(a), i.e., [5–8], show the average utility values of truthful user in Scenario (2) when k varies (1 and 2). In the left four bars of Fig. 3(a), the 1st/2nd bars and the 3rd/4th bars are experiment results without virtual budgets and with virtual budgets, respectively. As presented in Fig. 3(a), the results with virtual budget have approximately 0.1 higher utilities than the results without virtual budgets. Similarly, the right four bars of Fig. 3(a) (i.e., Scenario (2) which is without selfish user) have approximately 0.1 utility gaps between the results without virtual budgets and the results with virtual budgets while the results with virtual budgets take the highest. Overall, it can be interpreted that virtual budget has marginal impacts. However, we can observe clear impacts of virtual budget in Fig. 3(b). Fig. 3(b) shows the expected utility which will be obtained by truthful users in Scenario (1) and Scenario (2). Note that the left two bars, i.e., [1–2], are for Scenario (1) whereas the right two bars, i.e., [3–4], are for Scenario (2). As presented in the 1st bar of Fig. 3(b), the utility (calculated by $u_i = v_i - b_i$) becomes low when truthful user becomes winner since the second highest bid is high due to selfish user. However, it is very hard to bid with 8.35 (selfish user's bid value) consistently because selfish user participates in the trading by consuming its own virtual budget, as shown in the 2nd bar of Fig. 3(b). Thus, the selfish user will be eventually excluded from the trading because of dramatic budget degradation, and finally it cannot make any impacts on the remaining iterative auction procedure. In the right two bars of Fig. 3(b), relatively high utility values are observed since

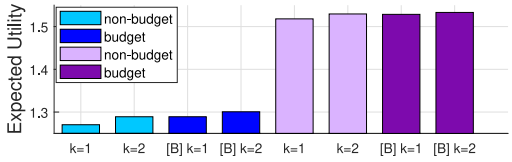

(a) Selfish bidder [1 – 4] and truthful bidder [5 – 8]

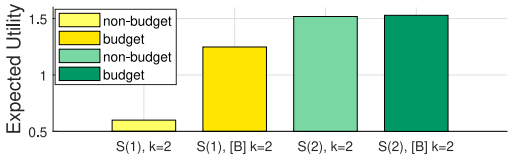

(b) Scenario (1) [1 – 2] and Scenario (2) [3 – 4]

Fig. 3. Average utility.
[B] $k = 1$ or [B] $k = 2$ stand for the experiments are performed when a *virtual budget* exists using the models with $k = 1$ or $k = 2$.

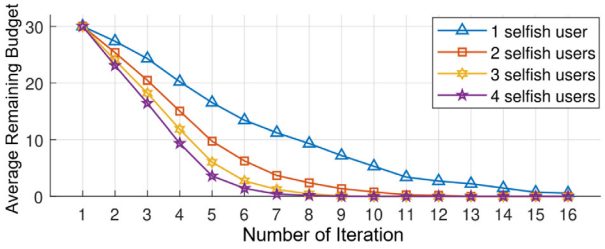

Fig. 4. Average remaining budget of selfish users when the number of selfish users increases in our framework.

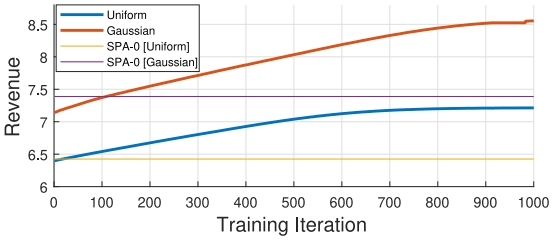

Fig. 5. Self-configurable natures in our proposed deep learning based auction in various distributions.

truthful users only exist. When the utility without and with virtual budgets is compared in Scenario (1), huge gap can be observed (≈0.7) which is the gain with truthful users. This experiment shows that selfish user cannot make significant impacts on our mechanism, thus its obvious truthful actions are eventually induced in our framework.

The performance evaluation results in Fig. 4 show the impacts on the average budgets of selfish users depending on the number of selfish users. This evaluation assumes that each selfish user has bid as 8.35 and also has 30 virtual budgets. As observed in Fig. 4, the proposed auction obviously excludes selfish users; and this exclusion speeds up when the number of selfish users increases. This means that selfish users more aggressively consume virtual budget as the number of selfish users increases. As presented in Fig. 4, the selfish user remains until 7.8, 4.8, 3.9, and 3.6 iterations (in average) when the numbers of selfish users are 1, 2, 3, and 4, respectively. This tendency can be analyzed that the second highest bid becomes larger when more selfish users involve in auction; and finally, the corresponding payment increases, thus the consumption of virtual budgets in selfish users increases.

Lastly, our software prototype conducts performance evaluation in terms of the self-configure natures in various user distributions (uniform vs. Gaussian) comparing to SPA-0. Fig. 5 shows the iteration counts for the convergence to optimal revenue. This result shows that the achieved revenues are 6.42 and 7.3 in SPA-0 and the proposed auction under uniform distribution, i.e., 13.7% higher performance gain. Similarly, the revenues are 7.38 and 8.53 in SPA-0 and the proposed auction under Gaussian distribution, i.e., 15.6% higher gain. Finally, it has been verified that our auction is self-configurable so that it conducts revenue optimal auction independent to environmental information.

5. Concluding remarks

In this paper, we proposed a trustworthy LEO handover decision mechanism using deep learning-based second price auction. According to the auction, one of LEO satellites will be selected to provide seamless Internet access services via bidding procedures under the consideration of received signal strength and service time. In addition, by utilizing deep learning framework, there are no needs to do analysis on environment information, i.e., self-configurable. As verified via software prototype based performance evaluation, following behaviors are observed, i.e., (i) the impacts of selfish users can be limited by defining virtual budgets for system stability, (ii) optimal revenue can be obtained via deep learning computation, and (iii) self-configurable operations can be realized for adapting various conditions.

Declaration of competing interest

The authors declare that they have no known competing financial interests or personal relationships that could have appeared to influence the work reported in this paper.

Acknowledgments

This work was supported by Electronics and Telecommunications Research Institute (ETRI) funded by the Korean government [21ZH1100, Research on 3D communication technology for hyper-connectivity].

References

[1] W. Lee, E. Kim, J. Kim, I. Lee, C. Lee, Movement-aware vertical handoff of WLAN and Mobile WiMAX for seamless ubiquitous access, IEEE Trans. Consum. Electron. 53 (4) (2007) 1268–1275.

[2] S. Park, J. Kim, Trends in LEO satellite handover algorithms, in: Proc. IEEE International Conference on Ubiquitous Future Networks, Jeju, Korea, 2021, pp. 422–425.

[3] J. Li, K. Xue, J. Liu, Y. Zhang, A user-centric handover scheme for ultra-dense LEO satellite networks, IEEE Wirel. Commun. Lett. 9 (11) (2020) 1904–1908.

[4] Y. Wu, G. Hu, F. Jin, J. Zu, A satellite handover strategy based on the potential game in LEO satellite networks, IEEE Access 7 (2019) 133641–133652.

[5] Y. Li, W. Zhou, S. Zhou, Forecast based handover in an extensible multi-layer LEO mobile satellite system, IEEE Access 8 (2020) 42768–42783.

[6] M. Shin, J. Kim, M. Levorato, Auction-based charging scheduling with deep learning framework for multi-drone networks, IEEE Trans. Veh. Technol. 68 (5) (2019) 4235–4248.

[7] H. Lee, S. Jung, J. Kim, Truthful electric vehicle charging via neural-architectural Myerson auction, ICT Express 7 (2) (2021) 196–199.

[8] S. Jung, W.J. Yun, M. Shin, J. Kim, J.-H. Kim, Orchestrated scheduling and multi-agent deep reinforcement learning for cloud-assisted multi-UAV charging systems, IEEE Trans. Veh. Technol. 70 (6) (2021) 5362–5377.

[9] S. Jung, J. Kim, M. Levorato, C. Cordeiro, J.-H. Kim, Infrastructure-assisted on-driving experience sharing for millimeter-wave connected vehicles, IEEE Trans. Veh. Technol. 70 (8) (2021) 7307–7321.

[10] H. Xu, D. Li, M. Liu, G. Han, W. Huang, C. Xu, QoE-driven intelligent handover for user-centric mobile satellite networks, IEEE Trans. Veh. Technol. 69 (9) (2020) 10127–10139.

[11] A. Ibrahim, A.S. Alfa, Using Lagrangian relaxation for radio resource allocation in high altitude platforms, IEEE Trans. Wireless Commun. 14 (10) (2015) 5823–5835.

[12] J. Thornton, D. Grace, M. Capstick, T. Tozer, Optimizing an array of antennas for cellular coverage from a high altitude platform, IEEE Trans. Wireless Commun. 2 (3) (2003) 484–492.

[13] O. Korçak, F. Alagöz, Virtual topology dynamics and handover mechanisms in earth-fixed LEO satellite systems, Comput. Netw. 53 (9) (2009) 1497–1511.

[14] R.B. Myerson, Optimal auction design, INFORMS Math. Oper. Res. 6 (1) (1981) 58–73.